

Facile synthesis of hollow microspherical $\text{YPO}_4\text{:Eu}^{3+}/\text{Tb}^{3+}$ using polystyrene spheres as sacrificial template and its photoluminescent properties

Yu Gao^{1,2,†}, Jinzhao Feng^{2,†}, Feixue Ai^{1,†}, Guiyan Zhao¹ ✉, Yanfeng Bi¹, Fu Ding², Yaguang Sun², Zhenhe Xu² ✉

¹College of Chemistry, Chemical Engineering and Environmental Engineering, Liaoning Shihua University, Fushun 113001, People's Republic of China

²The Key Laboratory of Inorganic Molecule-Based Chemistry of Liaoning Province, College of Applied Chemistry, Shenyang University of Chemical Technology, Shenyang 110142, People's Republic of China

[†]These authors contributed equally.

✉ E-mail: gyzhao@lnpu.edu.cn; xuzh@syuct.edu.cn

Published in Micro & Nano Letters; Received on 19th June 2017; Revised on 13th October 2017; Accepted on 12th January 2018

Monodisperse hollow microspherical $\text{YPO}_4\text{:Ln}^{3+}$ ($\text{Ln}^{3+} = \text{Eu}^{3+}/\text{Tb}^{3+}$) with diameters of around 2.5 μm have been successfully synthesised by combining a convenient homogeneous precipitation method, an ion exchange method, and a calcination process for the first time. X-ray diffraction, Fourier transform infrared, thermogravimetric analysis, scanning electron microscopy, transmission electron microscopy, and photoluminescence spectra were used to characterise the samples. Upon ultraviolet excitation, Eu^{3+} - and Tb^{3+} -doped microspherical YPO_4 showed typical red and green emission, respectively, which provide potential applications in bioanalysis, future colour displays, light-emitting devices, and so on.

1. Introduction: The fabrication of hollow micro/nanospheres with special functional properties (fluorescence, magnetism etc.), identically replicated in unlimited quantities in such a state that they can be manipulated, have attracted prodigious interest for their promising applications such as drug carrying [1–3], micro/nanoreactors [4, 5], catalysis [6, 7], long-duration energy storage [8–10], sensors [11], and so forth. These potentialities are mainly due to the unusual dependence of their high specific surface area, particular channel structure, and distinct low density [3]. From a simple point of view, hollow micro/nanospheres can be easily fabricated through digging void space inside solid spheres. However, such an operation is very difficult to achieve in the micro or nanoscale, and there are three major methods that are the most widely adopted to construct of hollow structures: (i) hard template method, (ii) soft template method, and (iii) self-template method. Among all three commonly used strategies, hard template method has been extensively adopted in the fabrication of hollow micro/nanospheres as it is straightforward to utilise and has advantages, such as control of size, shape, and structure [12–14]. It involves coating precursor onto the surface of template spheres, such as silica spheres, polymer latex particles, and carbon spheres, and subsequently removing the template spheres, getting hollow spheres [15, 16]. Heretofore, a lot of endeavours have been used in the preparation of hollow spheres, such as VOOH hollow spheres using $\text{V}(\text{OH})_2\text{NH}_2$ spheres as the template [17], GaN hollow spheres utilising SiO_2 as a template [18], TiO_2 hollow spheres through calcinating a carbon template [19, 20]. Despite these endeavours, it is challenging, yet highly desirable to exploit more efficient and facile methods to manufacture micro/nanospheres.

To date, the research on lanthanide-doped inorganic micro/nanomaterials has received considerable attention because they laid varying potential applications in lighting, display devices, photonic communication, magnetism, biology, catalysis, and solar energy [21–25]. Even more critically, luminescence property is of vital significance and has been investigating due to high monochromaticity, large Stokes shift, non-blinking, long lifetime, sharp fluorescence, rivalled traditional luminescent materials (organic dyes and quantum dots) [26–29]. It is worth noting that an ideal host

matrix needs high chemical and thermal stability, and low phonon energy to make sure good luminescence performance of Ln^{3+} activators. Among various host matrices, lanthanide orthophosphates (LnPO_4) have been potentially applied in phosphors [30], drug delivery [31], biolabelling [32], up-conversion materials [33], and so on. Among all lanthanide orthophosphates, yttrium orthophosphate (YPO_4) is a widely used fine host material for doping of rare earth ions to emit a wealth of colours. So far, multifarious morphologies of YPO_4 have been synthesised by different approaches, such as nanoparticles [34, 35], olivary architectures [36], rect-, hex-, and rod- YPO_4 nanocrystals [37], persimmon-like, cube-like architectures [38], and hexagonal submicropisms [30]. Yet, as far as we know, only a few of papers have been reported on the preparation of Ln^{3+} -doped YPO_4 hollow microspheres by templates method.

In this Letter, homogeneous $\text{YPO}_4\text{:Ln}^{3+}$ ($\text{Ln}^{3+} = \text{Eu}^{3+}/\text{Tb}^{3+}$) hollow microspheres with diameters of around 2.5 μm have been prepared by combining a convenient homogeneous precipitation approach, an ion exchange method, and a calcination process for the first time. We studied the structure, morphology, formation process, and luminescence properties of the as-obtained hollow YPO_4 microspheres. Moreover, our approach is economical, environmentally friendly, as well as beneficial to high yield mass production, which will provide a brilliant idea to prepare other hollow inorganic spherical materials and extend the widespread applications.

2. Experimental

2.1. Materials: The rare-earth oxides Ln_2O_3 (99.99%) ($\text{Ln} = \text{Y}$ and Eu) and Tb_4O_7 (99.99%) and other chemicals were purchased from Sinopharm Chemical Reagent Co., Ltd. All chemicals were analytical-grade reagents and used without further purification.

2.2. Preparation of the monodispersed polystyrene sphere (PS) microspheres: Monodisperse PS colloidal microspheres have been prepared by typical dispersion polymerisation [39]. In a typical synthesis, the poly(N-vinylpyrrolidone) stabiliser (1.0 g) was dissolved in ethanol (40 ml) in a three-necked round bottom flask, and then heated to 70°C under a nitrogen blanket and

purged with nitrogen for 2 h. Under vigorous stirring, a solution of azoisobutyronitrile (0.15 g) pre-dissolved in styrene monomer (15 g) was slowly added to the above reaction. The styrene polymerisation was maintained for 12 h before cooling to room temperature naturally. The product was purified by centrifugation, washed with ethanol, and then dried in a vacuum oven at 50°C.

2.3. Preparation of the monodisperse core-shell PS@Y(OH)CO₃ microspheres: About 1 mmol of YCl₃ aqueous solution and 100 mg of the as-prepared PS microspheres were added to 50 ml deionised water and well dispersed with the assistance of ultrasonication. Then, 2.0 g of urea was added to the above solution. The mixture solution was heated at 90°C for 2 h with vigorous stirring. The product was collected by centrifugation, and washed by deionised water and ethanol several times.

2.4. Preparation of the monodisperse YPO₄ hollow microspheres: The as-prepared PS@Y(OH)CO₃ sample was dispersed in water by ultrasonication. Then, 0.2 g of NH₄H₂PO₄ was dissolved in an 10 ml deionised water that was dropped into the solution by stirring. The mixing solution was then transferred into a Teflon bottle held in a stainless steel autoclave, sealed, and maintained at 180°C for 24 h. As the autoclave was cooled to room temperature naturally, the precipitate was separated by centrifugation, washed with deionised water and ethanol in sequence, and then dried in air at 80°C for 12 h. The final YPO₄ hollow microspheres were obtained through a heat treatment at 800°C in air for 4 h with a heating rate of 1°C min⁻¹. The Eu³⁺/Tb³⁺-doped YPO₄ hollow microspheres were prepared in a similar procedure except that by adding corresponding Eu₂O₃, and Tb₄O₇ together with Y₂O₃ as the starting materials as described above.

2.5. Characterisation: Powder X-ray diffraction (XRD) measurements were performed on a Rigaku-Dmax 2500 diffractometer with Cu Kα radiation (λ = 0.15405 nm). Fourier transform infrared (FTIR) spectra were measured with a Perkin-Elmer 580B infrared spectrophotometer with the KBr pellet technique. Thermogravimetric analysis (TGA) data was recorded with Thermal Analysis Instrument (SDT 2960, TA Instruments, New Castle, DE) with the heating rate of 10°C min⁻¹ in an air flow of 100 ml min⁻¹. The morphologies and composition of the as-prepared samples were inspected on a field emission scanning electron microscope (SU8010, Hitachi). Low- to high-resolution transmission electron microscopy (TEM) was performed using FEI Tecnai G2 S-Twin with a field emission gun operating at 200 kV. Images were acquired digitally on a Gatan multiplane CCD camera. The photoluminescence (PL) excitation and emission spectra were recorded with a Hitachi F-7000 spectrophotometer equipped with a 150 W xenon lamp as the excitation source. All measurements were performed at room temperature.

3. Results and discussion: The XRD results of the as-obtained PS spheres, the urea-assisted homogeneous precipitation product, the hydrothermal product, and final product after calcining at 800°C for 4 h are shown in Fig. 1. The as-obtained PS spheres show a diffraction peak at 19° (Fig. 1(a)) [13, 40]. The urea-assisted homogeneous precipitation product (PS@Y(OH)CO₃) shows two bands at 30° and 47° (Fig. 1(b)), which means that the as-obtained sample is amorphous. Fig. 1(c) shows the XRD pattern of the PS@YPO₄ sample that the PS@Y(OH)CO₃ sample was treated with NH₄H₂PO₄ in the hydrothermal process. All diffraction peaks are same as the tetragonal phase of YPO₄ (the standard card JCPDS Card No. 11-0254). However, the diffraction peaks of PS@YPO₄ sample are not strong and sharp, indicating that the PS@YPO₄ sample does not have high crystallinity. This could have an adverse effect on fluorescents because fewer traps and stronger luminescence are usually

resulted from high crystallinity. So the final calcination process has a double duty: remove the PS sphere template to form the hollow microspheres and increase the crystallinity. After the as-formed PS@YPO₄ was annealed at 800°C for 4 h, the position of the all peaks does not change (Fig. 1(d)).

The functional groups of the PS microspheres, the PS@Y(OH)CO₃ sample, the PS@YPO₄ sample, and the YPO₄ sample were identified by the FTIR spectra (Fig. 2). For the PS microspheres (Fig. 2(a)), the characteristic adsorption peaks at about 3200–2800, 1650–1300, and 600–850 cm⁻¹ are the stretching vibrations of aromatic C–H and C–C in-plane, and bending vibrations of aromatic C–C out-of-plane, respectively [41]. The FTIR spectrum of the PS@Y(OH)CO₃ sample (Fig. 2(b)) not only shows the characteristic peaks attributing to the PS microspheres, but also show the peaks at 1530, 1493, 1450, 1400, 1151, 1070, 1025, 844, and 760 cm⁻¹, corresponding to CO(v_{as}), CO (v_s),

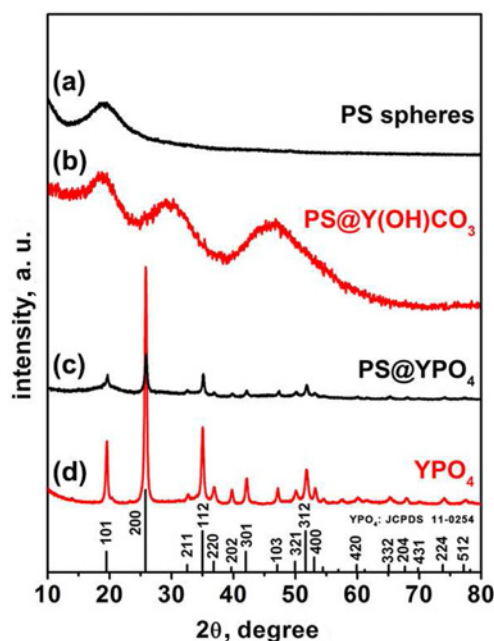


Fig. 1 XRD patterns of the PS spheres template, the core-shell PS@Y(OH)CO₃ microsphere, the core-shell PS@YPO₄ microsphere, and the YPO₄ hollow microsphere

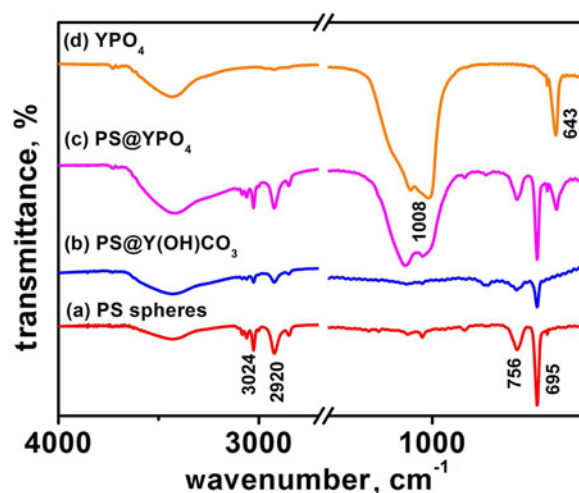


Fig. 2 FTIR spectra of the PS spheres template, the core-shell PS@Y(OH)CO₃ microsphere, the core-shell PS@YPO₄ microsphere, and the YPO₄ hollow microsphere

CO (δ), OH- (δ), and CO (δ), (ν_{as} =asymmetric stretch; ν_s =symmetric stretch; δ =deformation) [14], which indicate that the sample composed of PS and Y(OH)CO₃.

For the PS@YPO₄ sample (Fig. 2(c)), the bands at 643 and 1080 cm⁻¹ are the characteristic peaks of the phosphate groups [31], which indicates that the PS@Y(OH)CO₃ can convert to the PS@YPO₄ during the hydrothermal process. The YPO₄ sample (Fig. 2(d)) shows that all of the functional groups of the PS microspheres nearly disappear, and the characteristic adsorptions of the phosphate groups do not change, demonstrating that the PS template can thoroughly be removed by calcination.

The thermal behaviour of the PS microspheres and the PS@YPO₄ sample were further studied by TGA technique (Fig. 3). The TGA curve (Fig. 3(a)) of the PS microspheres displays one stage of 100% weight loss during the calcination process, which is the burning of PS spheres. The sample of PS@YPO₄ has two weight loss stages (Fig. 3(b)): a slow weight loss is the dehydration and densification of the PS microspheres. The other sharp weight loss should be ascribed to burning the PS microspheres template. Meanwhile, the percentage of residual weight is about 56.6%, which accounts for the final YPO₄ product, indicating that the hollow phosphors were prepared in considerably high yield by this method.

Figs. 4a and b show the scanning electron microscopy (SEM) and TEM images of the bare PS microspheres with diameters of around 2.10 μ m. Furthermore, the surface of the bare PS microspheres is very smooth. Figs. 4c and d reveal that the PS@Y(OH)CO₃ sample inherit the spherical morphology of the PS microspheres template. However, the surfaces of the PS@Y(OH)CO₃ sample are much rougher than that of the bare PS microspheres because of the precipitation of the Y(OH)CO₃ layers on the surface of PS microspheres. Furthermore, the size of PS@Y(OH)CO₃ sample is larger than the bare PS microspheres, with the size being increased from 2.10 to 2.5 μ m. So the shell is about 200 nm. Figs. 4e and f show the SEM and TEM images of the as-obtained PS@YPO₄ product such that the PS@Y(OH)CO₃ sample was treated with NH₄H₂PO₄ at 180°C for 12 h in the hydrothermal process. The size and core-shell structure were unchanged. However, its surfaces became roughened to some extent due to the aggregation of numerous formed nanorods with diameters of about 15 nm and lengths of about 30 nm.

After calcining at 800°C for 4 h, the YPO₄ product is composed of hollow microspheres with a diameter of around 2.5 μ m (Figs. 5a–d), which indicates that the PS microspheres template ultimately determine the morphology of the final product. More detailed structural information of hollow spherical YPO₄ sample is provided in the high-magnification SEM image (Fig. 5c). The broken YPO₄ microsphere demonstrates the hollow structure. A typical TEM image of the YPO₄ hollow microspheres further

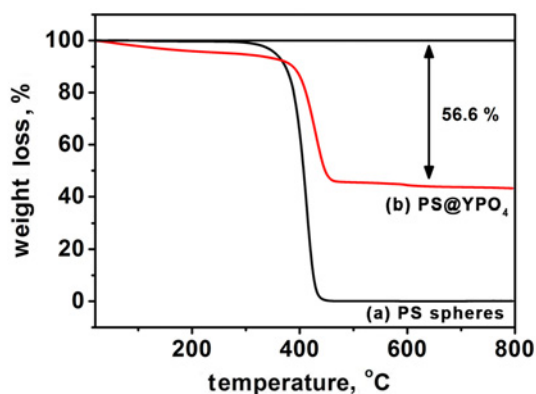


Fig. 3 TGA curves of the PS spheres template, and the core-shell PS@YPO₄ microsphere

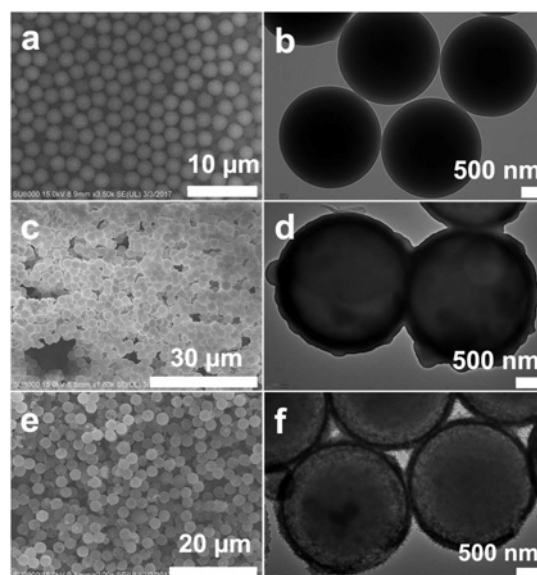


Fig. 4 SEM and TEM images
a, b PS spheres template
c, d Core-shell PS@Y(OH)CO₃ microsphere
e, f Core-shell PS@YPO₄ microsphere

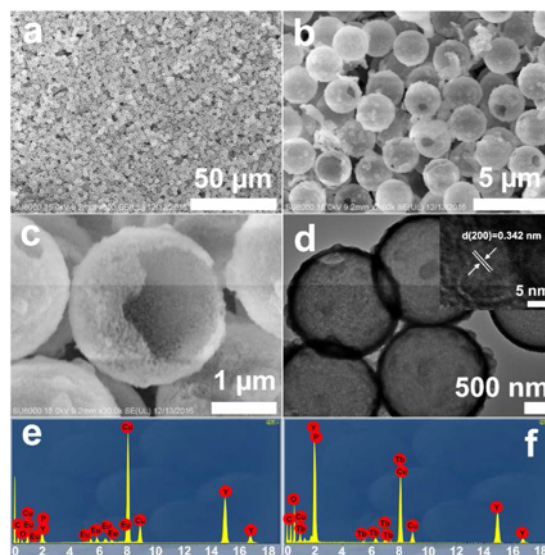
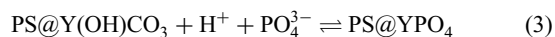
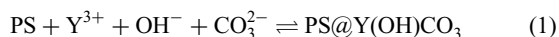


Fig. 5 SEM, TEM images, and EDX spectra
a–c SEM images of the YPO₄ hollow microsphere
d TEM image of the YPO₄ hollow microsphere. The inset is the HRTEM image of the core-shell PS@YPO₄ microsphere
e EDX spectrum of the YPO₄:Eu³⁺ hollow microsphere
f EDX spectrum of the YPO₄:Tb³⁺ hollow microsphere

verifies the homogenous size and hollow spherical structure of the YPO₄ (Fig. 5d). The HRTEM image (inset in Fig. 5d) shows that the interplanar distance between the adjacent lattice fringes is 0.342 nm, which can be indexed as the *d* spacing of the (200) plane of YPO₄ crystal. The chemical composition of the as-obtained YPO₄:Eu³⁺ and YPO₄:Tb³⁺ samples was further characterised by the energy-dispersive X-ray spectroscopy (EDX) analysis. The results show that no elements other than Y, Eu, P, O for YPO₄:Eu³⁺ (Fig. 5e) and Y, Tb, P, O for YPO₄:Tb³⁺ (Fig. 5f) are present from the measurement. Meanwhile, element mapping with a high-angle annular dark field and scanning transmission electron microscopy mode (HAADF-STEM) was used to further examine the elemental composition of YPO₄ hollow microspheres

(Fig. 6). It is observed that Y, P, and O elements are uniformly distributed in the shell of the hollow microspheres.

In order to reveal the formation process of YPO₄ hollow microsphere, a schematic illustration for the overall forming process is presented in Fig. 7. The PS microspheres were chosen as the template since they had a large number of functional groups with excellent hydrophilicity, which had a good affinity with Y³⁺, OH⁻, and CO₃²⁻. With the reaction proceeded, the Y(OH)CO₃ nuclei grew steadily and formed amorphous Y(OH)CO₃ layers on the surface of the PS microspheres, due to (1). In the second step, the PS@Y(OH)CO₃ core-shell microspheres were reacted with NH₄H₂PO₄ via the hydrothermal process to synthesise PS@YPO₄ core-shell microspheres. Due to (2), there were a lot of H⁺ and PO₄³⁻ ions in the reaction system, which could react with Y(OH)CO₃ to form YPO₄ layer on the surface of the PS microspheres (3). Finally, the PS spheres template was burned out through the calcination process, and the uniform hollow YPO₄ microspheres were obtained



As a good red-emitting activator, Eu³⁺ is widely used in the field of commercial phosphors, while the Tb³⁺ ions are commonly used as an activator in green phosphors. In our experiment, the PL properties of Eu³⁺- and Tb³⁺-doped YPO₄ microspheres were investigated. The doping ratio of Eu³⁺/Tb³⁺ ions is 5 mol% of Y³⁺ in

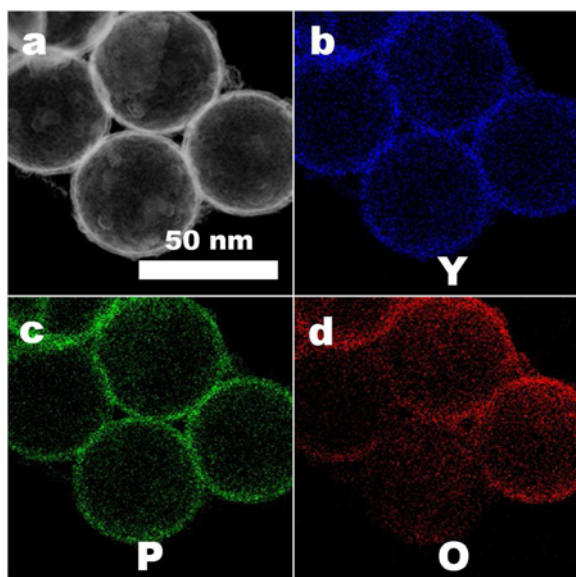


Fig. 6 HAADF-STEM images and the corresponding elemental maps
a YPO₄ hollow microsphere
b Y
c P
d O

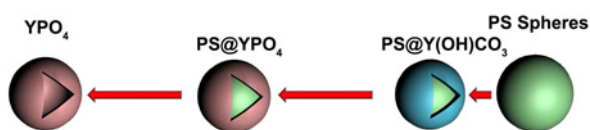


Fig. 7 Schematic illustration of formation of the YPO₄ hollow microsphere

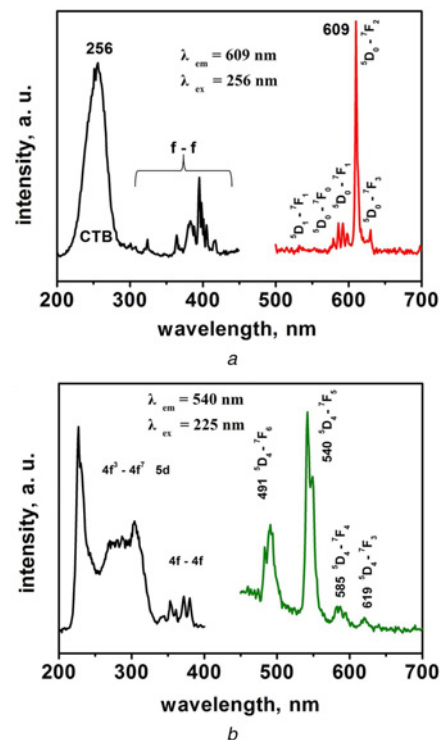


Fig. 8 Excitation and emission spectra
a YPO₄: 5 mol% Eu³⁺
b YPO₄: 5 mol% Tb³⁺

YPO₄. Fig. 8a shows the PL spectra of the YPO₄:Eu³⁺ hollow spheres. The excitation spectrum (Fig. 8a, left) of the YPO₄:Eu³⁺ sample composes of a strong band at 256 nm and a number of narrow bands between 300 and 450 nm, which can be ascribed to the charge transfer band (CTB) between the O²⁻ and Eu³⁺ ions and the *f-f* transitions within the Eu³⁺ 4f⁶ electron configuration, respectively. Upon excitation into the CTB of Eu³⁺ at 256 nm, the emission spectra of the YPO₄:Eu³⁺ sample consists of some peaks at 532, 578, 586, 592, 598, 609, and 628 nm, which can be attributed to ⁵D₀₋₇F_J (*J* = 1, 2, 3, 4) emission lines of the Eu³⁺ ions, respectively (Fig. 8a, right).

The excitation spectrum of YPO₄:Tb³⁺ sample consists of two bands in the 200–335 nm since the *f-d* transitions of Tb³⁺ in the YPO₄ lattice (Fig. 8b, left). Upon excitation into the transition at 226 nm, the emission spectrum (Fig. 8b, right) of YPO₄:Tb³⁺ sample shows the *f-f* transition lines within 4f⁸ electron configuration of Tb³⁺, such as ⁵D₄₋₇F₆ (491 nm), ⁵D₄₋₇F₅ (540 nm), ⁵D₄₋₇F₄ (585 nm), and ⁵D₄₋₇F₃ (619 nm). The strongest one is the ⁵D₄₋₇F₅ transition of Tb³⁺, located at 540 nm.

4. Conclusion: In summary, the novel YPO₄ hollow microspheres with diameters of around 2.5 μm have been successfully synthesised by the combination of a facile homogeneous precipitation approach, an ion-exchange process, and a calcination process. Since the synthetic process can be carried out at mild conditions, it should be straightforward to scale up the entire process for large-scale production of the YPO₄ hollow microspheres. Due to strong red/green emission of the YPO₄:Ln³⁺ (Ln³⁺ = Eu³⁺/Tb³⁺) hollow microspheres under the ultraviolet-visible light, these kinds of materials may have extensive potential applications in the areas of luminescence, disease therapy, and drug delivery according to their well-dispersed and homogeneous luminescent and hollow structure behaviours.

5. Acknowledgments: This work was supported by the National Natural Science Foundation of China (NSFC grant nos.

51402198, 21671139), the Natural Science Foundation of Liaoning Province (grant nos. 201602592, 20170540715), Educational Bureau of Liaoning Province for the Fundamental Research of Key Lab (grant nos. LZ2014028, LZ2016003), Talent Scientific Research/Scientific Research Cultivation Fund of LSHU (grant no. 2016XJJ-001/2016PY-014).

6 References

- [1] Xu Z., Ma P.A., Li C., *ET AL.*: 'Monodisperse core-shell structured up-conversion Yb(OH)CO₃@YbPO₄:Er³⁺ hollow spheres as drug carriers', *Biomaterials*, 2011, **32**, pp. 4161–4173
- [2] Yang P., Gai S., Lin J.: 'Functionalized mesoporous silica materials for controlled drug delivery', *Chem. Soc. Rev.*, 2012, **41**, pp. 3679–3698
- [3] Lv R., Gai S., Dai Y., *ET AL.*: 'Highly uniform hollow GdF₃ spheres: controllable synthesis, tuned luminescence, and drug-release properties', *ACS Appl. Mater. Interfaces*, 2013, **5**, pp. 10806–10818
- [4] Kim S.M., Jeon M., Kim K.W., *ET AL.*: 'Postsynthetic functionalization of a hollow silica nanoreactor with manganese oxide-immobilized metal nanocrystals inside the cavity', *J. Am. Chem. Soc.*, 2013, **135**, pp. 15714–15717
- [5] Zhang L., You H., Yang M., *ET AL.*: 'Core/shell Y(OH)CO₃:Eu³⁺/YBO₃:Eu³⁺ phosphors with sphericity, submicrometre size and nonaggregation characteristics', *Micro Nano Lett.*, 2011, **6**, pp. 728–731
- [6] Nguyen C.C., Vu N.N., Do T.-O.: 'Recent advances in the development of sunlight-driven hollow structure photocatalysts and their applications', *J. Mater. Chem. A*, 2015, **3**, pp. 18345–18359
- [7] Xu X., Zhang Z., Wang X.: 'Well-defined metal-organic-framework hollow nanostructures for catalytic reactions involving gases', *Adv. Mater.*, 2015, **27**, pp. 5365–5371
- [8] Moon G.D., Joo J.B., Dahl M., *ET AL.*: 'Nitridation and layered assembly of hollow TiO₂ shells for electrochemical energy storage', *Adv. Funct. Mater.*, 2014, **24**, pp. 848–856
- [9] Liu H., Li W., Shen D., *ET AL.*: 'Graphitic carbon conformal coating of mesoporous TiO₂ hollow spheres for high-performance lithium ion battery anodes', *J. Am. Chem. Soc.*, 2015, **137**, pp. 13161–13166
- [10] Xu Z., Liu Y., Ren F., *ET AL.*: 'Development of functional nanostructures and their applications in catalysis and solar cells', *Coord. Chem. Rev.*, 2016, **320–321**, pp. 153–180
- [11] Wang L., Lou Z., Fei T., *ET AL.*: 'Zinc oxide core-shell hollow microspheres with multi-shelled architecture for gas sensor applications', *J. Mater. Chem.*, 2011, **21**, pp. 19331–19336
- [12] Li W., Zheng X., Li F., *ET AL.*: 'Facile synthetic route to hollow gadolinium oxide spheres with tunable thickness', *Micro Nano Lett.*, 2012, **7**, pp. 1267–1269
- [13] Gao Y., Zhao Q., Fang Q., *ET AL.*: 'Facile fabrication and photoluminescence properties of rare-earth-doped Gd₂O₃ hollow spheres via a sacrificial template method', *Dalton Trans.*, 2013, **42**, pp. 11082–11091
- [14] Xu Z., Gao Y., Liu T., *ET AL.*: 'General and facile method to fabricate uniform Y₂O₃:Ln³⁺ (Ln³⁺=Eu³⁺, Tb³⁺) hollow microspheres using polystyrene spheres as templates', *J. Mater. Chem.*, 2012, **22**, pp. 21695–21703
- [15] Caruso F., Caruso R.A., Möhwald H.: 'Nanoengineering of inorganic and hybrid hollow spheres by colloidal templating', *Science*, 1998, **282**, pp. 1111–1114
- [16] Jia G., You H., Song Y., *ET AL.*: 'Facile synthesis and luminescence of uniform Y₂O₃ hollow spheres by a sacrificial template route', *Inorg. Chem.*, 2010, **49**, pp. 7721–7725
- [17] Wu C., Zhang X., Ning B., *ET AL.*: 'Shape evolution of new-phased lepidocrocite vooh from single-shelled to double-shelled hollow nanospheres on the basis of programmed reaction-temperature strategy', *Inorg. Chem.*, 2009, **48**, pp. 6044–6054
- [18] Sun X., Li Y.: 'Ga₂O₃ and GaN semiconductor hollow spheres', *Angew. Chem. Int. Ed.*, 2004, **43**, pp. 3827–3831
- [19] Wang H., Wu Z., Liu Y.: 'A simple two-step template approach for preparing carbon-doped mesoporous TiO₂ hollow microspheres', *J. Phys. Chem. C*, 2009, **113**, pp. 13317–13324
- [20] Caruso F., Shi X., Caruso R.A., *ET AL.*: 'Hollow titania spheres from layered precursor deposition on sacrificial colloidal core particles', *Adv. Mater.*, 2001, **13**, pp. 740–744
- [21] Gai S., Li C., Yang P., *ET AL.*: 'Recent progress in rare earth micro/nanocrystals: soft chemical synthesis, luminescent properties, and biomedical applications', *Chem. Rev.*, 2014, **114**, pp. 2343–2389
- [22] Xu Z., Quintanilla M., Vetrone F., *ET AL.*: 'Harvesting lost photons: plasmon and upconversion enhanced broadband photocatalytic activity in core@shell microspheres based on lanthanide-doped NaYF₄, TiO₂, and Au', *Adv. Funct. Mater.*, 2015, **25**, pp. 2950–2960
- [23] Wang F., Liu X.: 'Multicolor tuning of lanthanide-doped nanoparticles by single wavelength excitation', *Acc. Chem. Res.*, 2014, **47**, pp. 1378–1385
- [24] Wang J., Ming T., Jin Z., *ET AL.*: 'Photon energy upconversion through thermal radiation with the power efficiency reaching 16%', *Nat. Commun.*, 2014, **5**, p. 5669
- [25] Chatterjee D.K., Gnanasammandhan M.K., Zhang Y.: 'Small upconverting fluorescent nanoparticles for biomedical applications', *Small*, 2010, **6**, pp. 2781–2795
- [26] Wang C., Cheng L., Liu Y., *ET AL.*: 'Imaging-guided PH-sensitive photodynamic therapy using charge reversible upconversion nanoparticles under near-infrared light', *Adv. Funct. Mater.*, 2013, **23**, pp. 3077–3086
- [27] Tian B., Wang Q., Su Q., *ET AL.*: 'In vivo biodistribution and toxicity assessment of triplet-triplet annihilation-based upconversion nanocapsules', *Biomaterials*, 2017, **112**, pp. 10–19
- [28] Zeng S., Yi Z., Lu W., *ET AL.*: 'Simultaneous realization of phase/size manipulation, upconversion luminescence enhancement, and blood vessel imaging in multifunctional nanoprobes through transition metal Mn²⁺ doping', *Adv. Funct. Mater.*, 2014, **24**, pp. 4051–4059
- [29] Chen Z., Zheng W., Huang P., *ET AL.*: 'Lanthanide-doped luminescent nano-bioprobes for the detection of tumor markers', *Nanoscale*, 2015, **7**, pp. 4274–4290
- [30] Gao Z., Xiao Y., Wu D., *ET AL.*: 'Facile synthesis of GdPO₄:Eu³⁺ hierarchical hollow spheres via chemical conversion', *Micro Nano Lett.*, 2011, **6**, pp. 345–348
- [31] Xu Z., Cao Y., Li C., *ET AL.*: 'Urchin-like GdPO₄ and GdPO₄:Eu³⁺ hollow spheres – hydrothermal synthesis, luminescence and drug-delivery properties', *J. Mater. Chem.*, 2011, **21**, pp. 3686–3694
- [32] Yoon Y.-S., Lee B.-I., Lee K.S., *ET AL.*: 'Fabrication of a silica sphere with fluorescent and mr contrasting GdPO₄ nanoparticles from layered gadolinium hydroxide', *Chem. Commun.*, 2010, **46**, pp. 3654–3656
- [33] Heer S., Lehmann O., Haase M., *ET AL.*: 'Blue, green, and red upconversion emission from lanthanide-doped LuPO₄ and YbPO₄ nanocrystals in a transparent colloidal solution', *Angew. Chem. Int. Ed.*, 2003, **42**, pp. 3179–3182
- [34] Yan R., Sun X., Wang X., *ET AL.*: 'Crystal structures, anisotropic growth, and optical properties: controlled synthesis of lanthanide orthophosphate one-dimensional nanomaterials', *Chem. Eur. J.*, 2005, **42**, pp. 2183–2195
- [35] Grzyb T., Wiglusz R.J., Gruszczyńska A., *ET AL.*: 'Down- and up-converting dual-mode YPO₄:Yb³⁺, Tb³⁺ nanocrystals: synthesis and spectroscopic properties', *Dalton Trans.*, 2014, **43**, pp. 17255–17264
- [36] Yang M., You H., Guo N., *ET AL.*: 'Synthesis and luminescent properties of orderly YPO₄:Eu³⁺ olivary architectures self-assembled by nanoflakes', *CrystEngComm*, 2010, **12**, pp. 4141–4145
- [37] Huo Z., Chen C., Chu D., *ET AL.*: 'Systematic synthesis of lanthanide phosphate nanocrystals', *Chem. Eur. J.*, 2007, **13**, pp. 7708–7714
- [38] Qian L., Zhu J., Chen Z., *ET AL.*: 'Self-assembled heavy lanthanide orthovanadate architecture with controlled dimensionality and morphology', *Chem. Eur. J.*, 2009, **15**, pp. 1233–1240
- [39] Paine A.J., Luymes W., McNulty J.: 'Dispersion polymerization of styrene in polar solvents. 6. Influence of reaction parameters on particle size and molecular weight in poly (N-vinylpyrrolidone)-stabilized reactions', *Macromolecules*, 1990, **23**, pp. 3104–3109
- [40] Xu Z., Zhao Q., Sun Y., *ET AL.*: 'Synthesis of hollow La₂O₃:Yb³⁺/Er³⁺/Tm³⁺ microspheres with tunable up-conversion luminescence properties', *RSC Adv.*, 2013, **3**, pp. 8407–8416
- [41] Wang C., Yan J., Cui X., *ET AL.*: 'Synthesis of raspberry-like monodisperse magnetic hollow hybrid nanospheres by coating polystyrene template with Fe₃O₄@SiO₂ particles', *J. Colloid Interface Sci.*, 2011, **354**, pp. 94–99